Downloaded from orbit.dtu.dk on: May 05, 2023

DTU Library

Global patterns in marine predatory fish

van Denderen, Pieter Daniël; Lindegren, Martin ; MacKenzie, Brian; Watson, Reg; Andersen, Ken Haste

Published in:
Nature Ecology & Evolution

Link to article, DOI:
10.1038/s41559-017-0388-z

Publication date:
2018

Document Version
Peer reviewed version

Link back to DTU Orbit

Citation (APA):
van Denderen, P. D., Lindegren, M., MacKenzie, B., Watson, R., & Andersen, K. H. (2018). Global patterns in marine predatory fish. *Nature Ecology & Evolution*, *2*(1), 65-70. https://doi.org/10.1038/s41559-017-0388-z

General rights
Copyright and moral rights for the publications made accessible in the public portal are retained by the authors and/or other copyright owners and it is a condition of accessing publications that users recognise and abide by the legal requirements associated with these rights.

- Users may download and print one copy of any publication from the public portal for the purpose of private study or research.
- You may not further distribute the material or use it for any profit-making activity or commercial gain
- You may freely distribute the URL identifying the publication in the public portal

If you believe that this document breaches copyright please contact us providing details, and we will remove access to the work immediately and investigate your claim.

Global patterns in marine predatory fish

P. Daniël van Denderen[1*], Martin Lindegren[1], Brian R. MacKenzie[1], Reg A. Watson[2,3] and Ken H. Andersen[1]

[1]Centre for Ocean Life, National Institute of Aquatic Resources, Technical University of Denmark, Kemitorvet B-202, 2800 Kongens Lyngby, Denmark

[2]Institute for Marine and Antarctic Studies, University of Tasmania, GPO Box 252-49, Hobart, TAS, 7001, Australia

[3]Centre for Marine Socioecology, University of Tasmania, Hobart, Tasmania, 7004, Australia

Large teleost (bony) fish are a dominant group of predators in the oceans constituting a major source of food and livelihood for humans. These species differ markedly in morphology and feeding habits across oceanic regions; large pelagic species such as tunas and billfish typically occur in the tropics, whereas demersal species of gadoids and flatfish dominate boreal and temperate regions. Despite their importance for fisheries and the structuring of marine ecosystems, the underlying factors determining the global distribution and productivity of these two groups of teleost predators are poorly known. Here we show how latitudinal differences in predatory fish can essentially be explained by the inflow of energy at the base of the pelagic and benthic food chain. A low productive benthic energy pathway favours large pelagic species, whereas equal productivities support large demersal generalists that outcompete the pelagic specialists. Our findings demonstrate the vulnerability of large teleost predators to ecosystem-wide changes in energy flows and hence provide key insight to predict responses of these important marine resources under global change.

Marine top predators influence the structure and dynamics of food webs by imposing mortality and behavioural changes on prey and by feeding on parallel pathways of energy from both the pelagic (open water) and the benthic (bottom) zone of the ocean[1–3]. Many of these predator species have declined in population sizes and distribution ranges, which in several cases has resulted in large-scale changes in ecosystems, involving trophic cascades[2–4].

Large teleost fish are a dominant group of predators in the global oceans, support lucrative commercial and recreational fisheries and provide food for human populations worldwide[5–7]. These predators clearly differ in morphology and feeding habits across the world. In tropical and subtropical regions, teleost predators are often fast, mobile species that feed within the pelagic zone[8,9], while in boreal and

temperate regions the largest teleost species are typically slower growing, demersal (bottom-living)[10] and adapted to feeding on both pelagic and benthic organisms[6,11–14]. Despite their importance for structuring marine ecosystems and their significant socio-economic value, the underlying factors determining the global distribution and productivity of these two groups of marine predatory fish are poorly known. Here we test the specific hypothesis that spatial patterns in the distribution and productivity of these groups are primarily driven by pronounced global differences in the productivity of a pelagic and a benthic energy pathway in marine food webs worldwide (Fig. 1).

We examine this hypothesis by assessing the relative productivity of large marine teleost fishes using global fisheries landings data[15] across 232 marine ecoregions[16]. For each ecoregion, we calculate the average proportion of large pelagic vs demersal fish landings between 1970 and 2014. We show that in this case, the proportion of landings represents a good estimate of the dominant predatory feeding strategy in the sea. We develop a food-web model with two energy channels, one pelagic and one benthic, to formally test our hypothesis and to predict the biomass fraction of pelagic vs demersal predatory fish worldwide.

Results

The proportion of large pelagic and demersal teleost predators varied strongly in fisheries landings across the globe (Fig. 2). As expected, large pelagic fish dominate in the tropics and subtropics, while large demersal fish prevail in temperate and polar regions in both hemispheres. Despite the pronounced latitudinal gradients, some areas in the tropics have a relatively low proportion of large pelagic fish (e.g. Gulf of Mexico, Brazilian shelf), primarily due to high landings of demersal fish species; e.g. the highly abundant largehead hairtail (*Trichiurus lepturus*).

Whether landings data can predict biomass (and as such the dominant predatory fish feeding strategy in the sea) has been disputed[17]. Here, we use weight fractions in landings and do not predict absolute biomass. Nevertheless, average landings and biomass[18] are highly correlated for 71 pelagic and demersal predatory fish stocks (Supplementary Fig. 1, p-value <0.001, $r^2 = 0.78$). The weight fraction in landings also corresponds well to the fraction in biomass over time, based on assessed pelagic and demersal fish stocks[18] from nine different large marine ecosystems (LMEs) (Supplementary Fig. 2, p-value < 0.001, $r^2 = 0.91$). Proportions of pelagic and demersal fish landings weighted with the economic value of species[19] (i.e. a crude measure of potential fisheries preferences) demonstrate a similar global pattern (Supplementary Fig. 3, p-value < 0.001, $r^2 = 0.97$), highlighting that price differences between both groups are overshadowed by the considerably larger differences in the weight of the landings of the two groups. Further robustness checks show that the global patterns remain highly similar if large elasmobranches are included in the analysis (Supplementary Fig. 4, p-value < 0.001, $r^2 = 0.98$) or illegal, unregulated and unreported (IUU) catches and discards (p-value < 0.001, $r^2 = 0.99$). The robustness of our result to the potential biases described above provide strong support for using the weight fraction of pelagic vs demersal fish based on global landings as our response variable to estimate the dominant predatory fish feeding strategy in the sea.

We hypothesize that the relative production of pelagic and demersal predatory fish is dependent on the differences in inflow of energy at the base of the pelagic and benthic pathway (Fig. 1). Most of the ocean net primary production (NPP) occurs in the pelagic layer. Yet, in some regions, sufficient carbon reaches the bottom via sinking and other active transport processes to support high production of benthic organisms. There are multiple environmental conditions that can influence the downward flux of carbon to the seafloor. First, there is a clear relation with bathymetry, as in deeper oceans only a

77 fraction of the production from the pelagic zone may reach the seabed[20]. The proportion of NPP which
78 reaches the bottom also varies with latitude. This happens because low water temperatures decelerate
79 remineralization processes and subsequently increase the proportion of NPP available for export[21,22],
80 but also because seasonal variability in NPP may result in a temporal mismatch between phytoplankton
81 and zooplankton production leading to a larger fraction of (ungrazed) NPP sinking to the bottom during
82 the spring bloom in seasonal environments[23]. Finally, it has been suggested that the proportion of NPP
83 sinking to the seabed is dependent on the depth of the photic zone and either total NPP or chlorophyll
84 concentration[24].

85 We approximated the difference in pelagic and benthic production by calculating the ratio between the
86 fraction of NPP that remains in the photic zone (F_{photic})[24] versus the fraction of NPP that reaches the
87 seabed (F_{seabed}) (see Supplementary Fig. 5). Using non-linear regression models, we found that the ratio
88 between F_{photic} and F_{seabed} explains a substantial part of the global variability in the proportion of large
89 pelagic vs demersal fish landings (Fig. 3, deviance explained = 68%, p-value < 0.001; see other
90 environmental predictors in Supplementary Table 1). The results show how in most tropical and
91 subtropical areas a highly productive pelagic energy pathway favours large pelagic fish, while in many
92 temperate and polar regions more equal productivities of the two pathways favour large demersal fish
93 (feeding as a generalist on both pelagic and demersal resources).

94 In order to further test our hypothesis, we developed a food-web model with two energy channels to
95 predict the biomass fraction of large pelagic species across ecoregions (Fig. 1 and Supplementary Table
96 2-3). The pelagic and benthic energy pathways are modelled as two separate channels that have their
97 own resource carrying capacity. The carrying capacity of the pelagic resource is calculated by
98 multiplying a total resource carrying capacity constant (R_{max}) with F_{photic}, the carrying capacity of the

demersal resource was R_{max} . F_{seabed}. The resources are both preyed upon by an intermediate trophic level, representing smaller fishes and invertebrates, while two groups of predators are included at the top of the energy pathways; a pelagic specialist feeding exclusively on a pelagic diet, and a demersal generalist feeding on both energy pathways.

The food-web model predicted global patterns in pelagic vs demersal predators largely corresponding to the proportions of large pelagic fish derived from landings (Fig. 4a-b, $r^2 = 0.58$). However, some areas showed a strong mismatch between model predictions and landings data (Fig. 4b-c). Interestingly, the largest differences can be observed at high latitudes in the Southern Ocean and the temperate North Pacific where the model predicts a higher production of pelagic specialists compared to the proportions derived from landings. We expect that the model predictions are realistic because large pelagic predators are indeed present and highly abundant in many of these areas. However, not as predatory fish but as fast, pelagic-feeding endotherms that maintain a high body temperature and activity despite the cold waters. For example, the Aleutian Islands, Kamchatka shelf, Antarctica and South Georgia (Fig. 4c, red areas) harbour high biodiversity and densities of penguins and pinnipeds[25–27]. While this lends support to our model predictions, we stress the need for further research on the complementary roles of marine endo- and ectotherm predators. There is also a mismatch in ecoregions in the tropics where the model predicts higher production of demersal generalists compared to the proportions in landings (Fig. 4c, blue areas). In these regions, the energy fluxes to the seabed are predicted to be relatively high (Supplementary Fig. 5), thereby potentially supporting a high production of demersal generalists. The high fraction of NPP predicted to reach the seabed is consistent with other studies, using alternative methods, to predict the carbon flux to the seabed on a global scale[23]. In many of these areas, relatively high catch rates of sharks and rays can be observed[15], species that are often demersal

generalists and as such similar to demersal teleost predators. Although the contribution of large sharks and rays to overall fisheries landings is marginal (Supplementary Fig. 4), potentially the result of long-term overfishing[28], including elasmobranch predators in the analysis increases the amount of demersal generalists substantially near Australia, Peru and Chile in areas where the model predicts higher production of demersal generalists compared to the proportions in landings (Fig. 4c, Supplementary Fig. 4). An alternative explanation for the lower proportion of demersal generalists in the landings can be due to the ability of pelagic predators to disperse widely[9] and as such dampen local differences in fish abundances of the two predatory groups that have originated from variation in the energy flux to the seabed.

Discussion

Our study supports the hypothesis that the inflow of energy at the base of the pelagic and benthic channel determines the dominant feeding strategy of large teleost predatory fishes. Pelagic specialists dominate when energy is primarily channelled through the pelagic pathway, while demersal generalists outcompete the specialists when both pelagic and benthic resources are available. This explanation assumes that demersal generalists' niches and diets overlap with pelagic specialists because they exploit both benthic and pelagic resources. Overlapping diets have indeed been observed in areas where both groups of species co-occur[11,29,30]. Further, overlapping diets may occur even in the absence of direct spatial overlap between the predator groups, due to pronounced habitat shifts of pelagic prey species through daily (vertical) and seasonal (onshore-offshore) migrations (e.g.[31,32]). Since both large pelagic and demersal predators may access and feed on these highly mobile prey, but at different times, in different areas and even on different life stages, they engage in exploitative competition. Niche overlap will be lower in deep sea environments where demersal species are less able to exploit pelagic

resources. Even though reduced niche overlap in deep sea environments is not explicitly represented in our model or data analysis, it is implicitly captured because the fluxes are typically low in deep sea areas and consequently pelagic specialists are dominating. Although the degree of dietary overlap and the strength of competition between pelagic and demersal predators at a global scale are poorly known, our results suggest that competition between pelagic and demersal feeding strategies exists. Consequently, a decline in the productivity of the benthic energy pathway will shift dominance towards pelagic specialists (and vice versa).

We assumed that large pelagic teleost fish are superior in exploiting the pelagic resource compared to large demersal species. Large pelagic fish are highly adapted to feeding on fast-moving pelagic resources (such as forage fish) and have developed specific morphological features (e.g. high muscle protein, large gill surface area and the warming of muscles) to support an active pelagic lifestyle[33,34]. Such physiological and morphological adaptations can explain the superiority of pelagic specialists to feed on pelagic prey compared to the more "sluggish" demersal generalists. Yet, we lack knowledge to explicitly account for the energetic costs associated with these physiological and morphological adaptations[33] in a food-web model, and also, to account for the costs of finding, capturing and digesting prey for both groups of species. Quantifying these energetic costs will allow for a further refinement of the food-web model and support estimates of fish production of both species groups across oceanic regions.

Our global analysis of predatory fish largely ignored the role of non-teleost fish and marine endotherm predators. The contribution of non-teleost predators in global fisheries landings is low (Supplementary Fig. 4). Yet, non-teleost predators are typically overfished[28] and abundances were likely much higher in the past and may increase again in the future. The potential increase in abudance highlights the need to

understand the interplay between teleost and non-teleost predatory fish for future predictions of the global occurrence and productivity of fish predators. Aditionally, it is unclear from our study under which environmental conditions endotherm predators are a highly abundant and dominant predatory species group. Following the results of our food-web analysis (Fig. 4), we hypothesized that pelagic-feeding endotherms are the dominant predatory group at high latitudes in the Southern Ocean and the temperate North Pacific. Yet, the complementary roles of marine endo- and ectotherm predators in relation to temperature and the productivity of the pelagic and benthic energy pathways needs further study.

When top predators feed on both pelagic and benthic prey resources, they act as couplers of these energy pathways. This coupling may infer stability to the food web if the predators balance the strength of their feeding interactions on pelagic and benthic prey with the relative difference in productivity (and turnover rates) of the pathways[1]. We argue that not all predatory fish act as such "balanced" couplers, as species can be specialized on exploiting pelagic resources. The specialization implies that ecosystem-level variations in the productivity of the pelagic and benthic energy pathways will not only affect the occurrence and productivity of large predatory fishes, but also the stability of the ecosystem.

There is large uncertainty related to current predictions of future fish and fisheries production, primarily since it is unclear how climate change will affect ocean primary production and how energy will be transferred to the upper trophic levels of marine ecosystems[35,36]. Our findings suggest that changes in the global occurrence and productivity of large predatory fishes can be anticipated by understanding how climate change will affect the base of pelagic and benthic food chains. Changes in the productivity of these energy pathways in response to climate change are expected[37,38] and, in some instances, already observed, e.g. large-scale changes in phytoplankton abundance and ocean primary

187 production[39,40]. For most continental shelf areas, climate change has been predicted to decrease detritus
188 fluxes to the seafloor[35], thereby potentially limiting large demersal fish abundances and fisheries
189 production. Accounting for the changes in the pelagic and demersal energy pathways is therefore key to
190 reliably predict the effects of climate change on the upper trophic levels of marine ecosystems, and the
191 impact on supported fisheries.

192 **Method**

193 Global fisheries data

194 We used global fisheries landings data[15] to determine general patterns in feeding strategies of marine
195 predatory fish between 1970 and 2014. The spatial fisheries landings data is predominately from global
196 fisheries catch statistics assembled by the Food and Agriculture Organization of the United Nations
197 (FAO) and complemented by statistics from various international and national agencies. These datasets,
198 with higher spatial resolution, were nested into the broader FAO regions, replacing the data reported at
199 the coarser spatial resolution. The global fisheries landings data was mapped to 30-min spatial cells
200 using information on the distribution of reported taxa and fishing fleets[15]. For the purpose of this study,
201 we aggregated the data and examined fisheries landings data on a marine ecoregion scale[16].

202 Feeding strategies of marine fish

203 To examine the productivity of marine teleost fish along the pelagic and benthic energy pathways, we
204 classified fish into two general feeding strategies, either feeding exclusively on the pelagic pathway
205 (pelagic fish) or (partly) relying on the benthic pathway for feeding (demersal fish). This was done
206 using the functional group classification system developed in the Sea Around Us (SAU) project[41]. Data
207 classified using the SAU project as shark, ray, any type of invertebrate or bathydemersal and
208 bathypelagic fish (these groups include the mesopelagic fish) were removed (see Supplementary Table
209 4). This limited our analysis to teleost fish and the two dominant feeding strategies. The two feeding
210 strategies were further divided on the basis of fish maximum size[42]. Large predatory species were
211 classified as fish with a maximum size $\geq$ 90 cm. The choice of this maximum size limit did not affect
212 our analysis as it can range from 70 – 150 cm without changing the results (Supplementary Fig. 6). Part
213 of the fisheries landings has not been identified (e.g. marine animals, marine fishes not identified) and

these observations were excluded. Other data are identified at too general a taxonomic grouping to derive the correct size-class (e.g. Gadiformes, Gadidae) and these landings data were assumed to represent species with smaller maximum sizes than 70 cm.

For each of the ecoregions, we calculated the average weight fraction of pelagic fish compared to demersal fish in the fisheries landings data between 1970 and 2014. This was only done for ecoregions where at least 60% of the landings data (in tonnes) could be classified into one of the functional groups from the SAU project (but note that the main findings are unaffected when more or less strict criteria for ecoregion selection are chosen). All fractions were averaged over at least 24 years of data (for 219 ecoregions fractions were averaged over 45 years of data).

Besides the large predatory teleost fish, we also determined whether there were general patterns in feeding strategies of teleost fish species with a maximum size < 90 cm (Supplementary Fig. 7). The results show there is no clear latitudinal pattern and no relationship between the small pelagic fish fraction and F_{photic}/F_{seabed}. The pattern is not improved when pelagic and benthic invertebrate landings are included in the analysis (Supplementary Fig. 7).

Potential bias due to the use of fisheries landings

Our assessment of the global variation in the large predatory fish may be biased by our use of global fisheries landings data instead of biomass data. We included a variety of analyses to examine this potential bias. We first examined with available stock assessments from the RAM Legacy Stock Assessment database[18], the relationship between catch and biomass of large teleost fish. For this analysis, data was available for 71 different large predatory fish stocks (38 pelagic and 33 demersal, Supplementary Table 5). For each stock, we averaged both total biomass and total catch for all years with assessment data and examined across stocks the relationship between average biomass and catch

and whether this differs between both feeding groups (model comparison using AIC scores). Afterwards, we tested the relationship between the weight fraction of pelagic fish versus demersal fish in catch and biomass over time. This was done by selecting pelagic and demersal fish in all size groups from the RAM stock assessment database[18] for nine different Large Marine Ecosystems (LMEs) over multiple years. The LMEs and years are selected since they have data available on assessed fish stocks in both feeding strategies (see Supplementary Table 6). To further check robustness of our findings, we examined how much the fraction large pelagic and demersal fish varied when the fraction is corrected for the economic value of the species (assuming that species are preferred by fisheries when they have higher economic value). Nominal economic value, standardized per unit weight, were derived for each species and year from Sumaila et al.[19], and were used to estimate the economic value of both feeding groups (standardized per unit weight) per ecoregion and year. When multiple species from the same feeding group were present in the landings in a particular ecoregion and year, the economic value of that feeding group was averaged by weighting all species with the landings. Afterwards, we calculated the price difference between pelagic and demersal fish for each year and ecoregion and averaged this across all years per ecoregion. A price-corrected weight fraction large pelagic fish was then calculated by: wf . (1-pf) / (wf . (1-pf) + (1-wf) . pf), where wf is the weight fraction large pelagic fish from fisheries landings and pf is the price fraction (a fraction of 0.9 means that pelagic fish are 9 times more valuable than demersal fish at similar tonnes of landings) (Supplementary Fig. 3). We also examined how the inclusion of large sharks and rays (taken from the fisheries landings database[15]) affected the global patterns in predatory fish. Classification of pelagic (oceanic) sharks and rays followed[43], all other taxa were classified as demersal generalists (maximum body size is based on[42]). Finally, we examined how estimates of illegal, unregulated and unreported (IUU) catches and discarded fish affected our calculation of the weight fraction of large pelagic vs demersal fish. Estimates of IUU

catches and discarded fish were taken from the spatial fisheries landings database[15] per ecoregion and year.

Pelagic and benthic energy production

We hypothesized that the relative production of pelagic and demersal fish in fisheries landings across ecoregions is dependent on the differences in pelagic and benthic production. We approximated the difference in production by calculating the ratio between the fraction of NPP that remains in the photic zone (F_{photic}) versus the fraction of NPP that sinks to the seabed (F_{seabed}). This was done by first calculating the fraction of NPP that sinks out of the photic zone (*pe*-ratio) and secondly by accounting for energy loss between the depth of the photic zone and the seabed.

We used an empirical relationship introduced by Dunne et al.[24] to calculate the *pe*-ratio. This relationship captures ~60% of observed global variation in *pe*-ratio using field-derived estimates of sea surface temperature (SST), primary production (NPP) and the photic zone depth (Zeu). In this calculation, increased temperature reduces the *pe*-ratio, while it is increased with increasing primary production and a smaller photic zone depth: $\text{pe-ratio} = -0.0101\text{SST} + 0.0582\ln\left(\frac{\text{NPP}}{\text{Zeu}}\right) + 0.419$. To estimate the *pe*-ratio on a global scale with the empirical model, we used average annual sea surface temperature (degrees Celsius) between 1998 and 2008 (http://www.esrl.noaa.gov/psd/data/gridded/data.noaa.oisst.v2.html), average daily net primary production (mg C / m^2 / day) from the Vertically Generalized Production Model (VGPM) using MODIS data between 2003 and 2008 (http://www.science.oregonstate.edu/ocean.productivity)[44] and we approximated the photic zone depth from average daily surface chlorophyll-a concentrations (mg Chl / m^3 / day) from the Sea-viewing Wide Field of view Sensor (SeaWiFS) between 1998 and 2008 (http://oceancolor.gsfc.nasa.gov/cms) (following[45], see for original description[46]). The sea surface

temperature data was resampled to a 1/12 degrees grid to be able to use more detailed information on spatial variation in bathymetry. The derived *pe*-ratios varied across the globe between 0.04 and 0.74 and were used to calculate F_{photic} (Supplementary Fig. 5), the predicted fraction of NPP that remains in the photic zone:

$$F_{\text{photic}} = 1 - r,$$

where r is the *pe*-ratio.

The fraction of NPP that sinks out of the photic zone is reduced in energetic content before it reaches the seabed, especially in deeper oceans where only a fraction of the production from the pelagic zone may reach the seabed. To account for this effect, we accounted for energy loss, adjusting a function described in[47]:

For all grid cells where the seabed depth is equal or shallower than depth of the photic zone:

$$F_{\text{seabed}} = pe\text{-ratio},$$

all other grid cells:

$$F_{\text{seabed}} = pe\text{-ratio (seabed depth / depth photic zone)}^{-0.86}$$

Bathymetric data (m) was extracted per 1/12 degrees grid from the ETOPO1 Global Relief Model with sea ice cover[48].

The calculated fluxes in the pelagic and benthic zone only provide a first-approximation of the relative productivity of the pathways. The estimates ignore different aspects well-known to influence pelagic and benthic energy pathways, such as the role of benthic primary producers, which especially in

coastal waters contribute to a large part of the overall production[49], areas with high subsurface productivity, where NPP is underestimated when using satellite-derived NPP products[50,51], and any active transport processes to the seafloor[52,53]. Despite these limitations, the predicted large-scale spatial variation in F_{photic} and F_{seabed} (Supplementary Fig. 5) seems to be consistent with other studies, using alternative methods[23,54].

Data aggregation per ecoregion and data analysis

Both F_{photic} and F_{seabed} were averaged per ecoregion. To account for latitudinal differences in grid size all F_{photic} and F_{seabed} values per ecoregion were weighted with respect to latitude (weighting factor = $\cos(\pi/180 \cdot \text{degrees latitude})$) following[55]. Besides, as fish production is expected to be highest in areas with high primary production[56], we also weighted F_{photic} and F_{seabed} per ecoregion with respect to grid cell differences in NPP.

Relationships between the fraction of pelagic fish and the ratio between F_{photic} and F_{seabed} were examined using generalized additive models with a beta distribution (continuous probability distribution between 0 and 1) and (after model fit inspection) with a cauchit link function. The ratio between F_{photic} and F_{seabed} was $\log_{10}$ transformed, while the pelagic fish fraction was transformed to avoid zeros and ones following[57]; $y = (y(n-1)+0.5)/n$, where y is the pelagic fish fraction and n the number of ecoregions. Maps were produced using rworldmap[58].

Food-web model

Following the results of the fisheries data analyses, a food-web model was developed to study the competitive interactions between large pelagic specialists and demersal generalists across marine ecoregions. The benthic and pelagic energy pathways were modelled as two separate channels that

have their own resource carrying capacities with semi-chemostat dynamics. The carrying capacity of the pelagic resource (K_p) was calculated by multiplying the total resource carrying capacity (R_{max}) with F_{photic}, the carrying capacity of the demersal resource (K_B) was R_{max} . F_{seabed} (see for model formulation Supplementary Table 2). The resources were both preyed upon by an intermediate trophic level, while two predatory species were included at the top of the energy pathways (following Fig. 1).

We hypothesized that large pelagic teleost fish are superior in exploiting the pelagic resource compared to large demersal species (see for arguments the second paragraph in the discussion section). To incorporate this in the model, feeding as a generalist comes at a cost and this cost was implemented with a lower attack rate of the generalist, meaning that the specialist is superior in exploiting the pelagic resource. The value of the attack rate parameter was selected to obtain (approximately) an equal amount of ecoregions that either overestimated the amount of pelagic or demersal fish compared to fisheries landings. It resulted in an attack rate of the generalist that is 0.8 of the attack rate of the specialist. This value can be varied between 0.65 and 0.95 without changing the r^2 of the statistical relationship between landings data and model output with 4% (r^2 is 58% when a value of 0.8 is used, see Fig. 4).

Data availability:

A table is available as supplementary data with information per ecoregion on the fraction pelagic fish in landings, environmental variables and the food-web model outcome. Detailed global fisheries landings data is available from Watson[15].

References

1. Rooney, N., McCann, K., Gellner, G. & Moore, J. C. Structural asymmetry and the stability of diverse food webs. *Nature* **442,** 265–269 (2006).

2. Estes, J. A., Heithaus, M., McCauley, D. J., Rasher, D. B. & Worm, B. Megafaunal impacts on structure and function of ocean ecosystems. *Annu. Rev. Environ. Resour.* **41,** 83–116 (2016).

3. Heithaus, M. R., Frid, A., Wirsing, A. J. & Worm, B. Predicting ecological consequences of marine top predator declines. *Trends Ecol. Evol.* **23,** 202–210 (2008).

4. Baum, J. K. & Worm, B. Cascading top-down effects of changing oceanic predator abundances. *J. Anim. Ecol.* **78,** 699–714 (2009).

5. FAO. *The State of World Fisheries and Aquaculture 2016. Contributing to food security and nutrition for all. Rome. 200 pp.* (2016).

6. Link, J. S., Bogstad, B., Sparholt, H. & Lilly, G. R. Trophic role of Atlantic cod in the ecosystem. *Fish Fish.* **10,** 58–87 (2009).

7. Sibert, J., Hampton, J., Kleiber, P. & Maunder, M. Biomass, size, and trophic status of top predators in the Pacific Ocean. *Science* **314,** 1773–1776 (2006).

8. Boyce, D. G., Tittensor, D. P. & Worm, B. Effects of temperature on global patterns of tuna and billfish richness. *Mar. Ecol. Prog. Ser.* **355,** 267–276 (2008).

9. Worm, B. & Tittensor, D. P. Range contraction in large pelagic predators. *Proc. Natl. Acad. Sci.* **108,** 11942–11947 (2011).

10. Pauly, D., Watson, R. & Alder, J. Global trends in world fisheries: impacts on marine ecosystems and food security. *Philos. Trans. Biol. Sci.* **360,** 5–12 (2005).

11. Garrison, L. P. & Link, J. S. Dietary guild structure of the fish community in the Northeast United States continental shelf ecosystem. *Mar. Ecol. Prog. Ser.* **202,** 231–240 (2000).

12. Bulman, C., Althaus, F., He, X., Bax, N. J. & Williams, A. Diets and trophic guilds of demersal fishes of the south-eastern Australian shelf. *Mar. Freshw. Res.* **52,** 537–548 (2001).

13. Byron, C. J. & Link, J. S. Stability in the feeding ecology of four demersal fish predators in the US Northeast Shelf Large Marine Ecosystem . *Mar. Ecol. Prog. Ser.* **406,** 239–250 (2010).

14. López-López, L. *et al.* Is juvenile anchovy a feeding resource for the demersal community in the Bay of Biscay? On the availability of pelagic prey to demersal predators. *ICES J. Mar. Sci.* **69,** 1394–1402 (2012).

15. Watson, R. A. A database of global marine commercial, small-scale, illegal and unreported fisheries catch 1950–2014. *Sci. data* **4,** 170039 (2017).

16. Spalding, M. D. *et al.* Marine ecoregions of the world: a bioregionalization of coastal and shelf areas. *Biosci.* **57,** 573–583 (2007).

17. Branch, T. A. *et al.* The trophic fingerprint of marine fisheries. *Nature* **468,** 431–435 (2010).

18. Ricard, D., Minto, C., Jensen, O. P. & Baum, J. K. Examining the knowledge base and status of commercially exploited marine species with the RAM Legacy Stock Assessment Database. *Fish Fish.* **13,** 380–398 (2012).

19. Sumaila, U. R., Marsden, A. D., Watson, R. & Pauly, D. A global ex-vessel fish price database: construction and applications. *J. Bioeconomics* **9,** 39–51 (2007).

20. Suess, E. Particulate organic carbon flux in the oceans-surface productivity and oxygen utilization. *Nature* **288,** 260–263 (1980).

21. Pomeroy, L. R. & Deibel, D. O. N. Temperature regulation of bacterial activity during the spring bloom in Newfoundland Coastal Waters. *Science* **233,** 359–361 (1986).

22. Laws, E. A., Falkowski, P. G., Smith, W. O., Ducklow, H. & McCarthy, J. J. Temperature effects on export production in the open ocean. *Global Biogeochem. Cycles* **14,** 1231–1246 (2000).

23. Lutz, M. J., Caldeira, K., Dunbar, R. B. & Behrenfeld, M. J. Seasonal rhythms of net primary production and particulate organic carbon flux to depth describe the efficiency of biological pump in the global ocean. *J. Geophys. Res.* **112,** C10011 (2007).

24. Dunne, J. P., Armstrong, R. A., Gnanadesikan, A. & Sarmiento, J. L. Empirical and mechanistic models for the particle export ratio. *Global Biogeochem. Cycles* **19,** GB4026 (2005).

25. Tittensor, D. P. *et al.* Global patterns and predictors of marine biodiversity across taxa. *Nature* **466,** 1098–1101 (2010).

26. Mackintosh, N. A. The pattern of distribution of the Antarctic fauna. *Proc. R. Soc. B. Biol. Sci.* **152,** 624–631 (1960).

27. Kaschner, K., Tittensor, D. P., Ready, J., Gerrodette, T. & Worm, B. Current and future patterns of global marine mammal biodiversity. *PLoS One* **6,** e19653 (2011).

399 28. Davidson, L. N. K., Krawchuk, M. A. & Dulvy, N. K. Why have global shark and ray landings
400 declined: improved management or overfishing? *Fish Fish.* **17,** 438–458 (2016).

401 29. Drapeau, L., Pecquerie, L., Fréon, P. & Shannon, L. J. Quantification and representation of
402 potential spatial interactions in the southern Benguela ecosystem. *African J. Mar. Sci.* **26,** 141–
403 159 (2004).

404 30. Brodeur, R. D., Buchanan, J. C. & Emmett, R. L. Pelagic and demersal fish predators on juvenile
405 and adult forage fishes in the Northern California Current: spatial and temporal variations.
406 *CalCOFI Rep.* **55,** 96–116 (2014).

407 31. McDaniel, J., Piner, K., Lee, H. H. & Hill, K. Evidence that the migration of the northern
408 subpopulation of Pacific Sardine (*Sardinops sagax*) off the west coast of the United States is
409 age-based. *PLoS One* **11,** e0166780 (2016).

410 32. Varpe, Ø., Fiksen, Ø. & Slotte, A. Meta-ecosystems and biological energy transport from ocean
411 to coast: the ecological importance of herring migration. *Oecologia* **146,** 443 (2005).

412 33. Killen, S. S. *et al.* Ecological influences and morphological correlates of resting and maximal
413 metabolic rates across teleost fish species. *Am. Nat.* **187,** 592–606 (2016).

414 34. Watanabe, Y. Y., Goldman, K. J., Caselle, J. E., Chapman, D. D. & Papastamatiou, Y. P.
415 Comparative analyses of animal-tracking data reveal ecological significance of endothermy in
416 fishes. *Proc. Natl. Acad. Sci.* **112,** 6104–6109 (2015).

417 35. Stock, C. A. *et al.* Reconciling fisheries catch and ocean productivity. *Proc. Natl. Acad. Sci.* **114,**
418 E1441–E1449 (2017).

36. Brander, K. M. Global fish production and climate change. *Proc. Natl. Acad. Sci.* **104,** 19709–19714 (2007).

37. Capotondi, A., Alexander, M. A., Bond, N. A., Curchitser, E. N. & Scott, J. D. Enhanced upper ocean stratification with climate change in the CMIP3 models. *J. Geophys. Res. Ocean.* **117,** C04031 (2012).

38. Sarmiento, J. L. *et al.* Response of ocean ecosystems to climate warming. *Global Biogeochem. Cycles* **18,** GB3003 (2004).

39. Richardson, A. J. & Schoeman, D. S. Climate impact on plankton ecosystems in the Northeast Atlantic. *Science* **305,** 1609–1612 (2004).

40. Behrenfeld, M. J. *et al.* Climate-driven trends in contemporary ocean productivity. *Nature* **444,** 752–755 (2006).

41. Pauly, D. & Zeller, D. Sea Around Us concepts, design and data. (2015). *www.seaaroundus.org*

42. Froese, R. & Pauly, D. FishBase. *www.fishbase.org* (2016).

43. Compagno, L. J. V. Pelagic elasmobranch diversity. Ch. 3 in *Sharks of the open Ocean: biology, fisheries and conservation* ed. Camhi, M. D., Pikitch, E. K. & Babcock, E. A. (Blackwell Publ. Ltd., 2008).

44. Behrenfeld, M. J. & Falkowski, P. G. Photosynthetic rates derived from satellite-based chlorophyll concentration. *Limnol. Oceanogr.* **42,** 1–20 (1997).

45. Friedland, K. D. *et al.* Pathways between primary production and fisheries yields of Large

Marine Ecosystems. *PLoS One* **7,** e28945 (2012).

46. Morel, A. & Berthon, J.-F. Surface pigments, algal biomass profiles, and potential production of the euphotic layer: relationships reinvestigated in view of remote-sensing applications. *Limnol. Oceanogr.* **34,** 1545–1562 (1989).

47. Martin, J. H., Knauer, G. A., Karl, D. M. & Broenkow, W. W. VERTEX: carbon cycling in the northeast Pacific. *Deep Sea Res. Part A. Oceanogr. Res. Pap.* **34,** 267–285 (1987).

48. Amante, C. & Eakins, B. ETOPO1 1 arc-minute global relief model: procedures, data sources and analysis. (2009).

49. Ward, C. L., McCann, K. S. & Rooney, N. HSS revisited: multi-channel processes mediate trophic control across a productivity gradient. *Ecol. Lett.* **18,** 1190–1197 (2015).

50. Richardson, K., Visser, A. W. & Pedersen, F. B. Subsurface phytoplankton blooms fuel pelagic production in the North Sea. *J. Plankton Res.* **22,** 1663–1671 (2000).

51. Schulien, J. A., Behrenfeld, M. J., Hair, J. W., Hostetler, C. A. & Twardowski, M. S. Vertically-resolved phytoplankton carbon and net primary production from a high spectral resolution lidar. *Opt. Express* **25,** 13577–13587 (2017).

52. Jónasdóttir, S. H., Visser, A. W., Richardson, K. & Heath, M. R. Seasonal copepod lipid pump promotes carbon sequestration in the deep North Atlantic. *Proc. Natl. Acad. Sci.* **112,** 12122–12126 (2015).

53. Davison, P. C., Checkley, D. M., Koslow, J. A. & Barlow, J. Carbon export mediated by mesopelagic fishes in the northeast Pacific Ocean. *Prog. Oceanogr.* **116,** 14–30 (2013).

458 54. Siegel, D. A. *et al.* Global assessment of ocean carbon export by combining satellite
459 observations and food-web models. *Global Biogeochem. Cycles* **28,** 181–196 (2014).

460 55. Belkin, I. M. Rapid warming of large marine ecosystems. *Prog. Oceanogr.* **81,** 207–213 (2009).

461 56. Jennings, S. & Collingridge, K. Predicting consumer biomass, size-structure, production, catch
462 potential, responses to fishing and associated uncertainties in the world's marine ecosystems.
463 *PLoS One* **10,** e0133794 (2015).

464 57. Smithson, M. & Verkuilen, J. A better lemon squeezer? Maximum-likelihood regression with
465 beta-distributed dependent variables. *Psychol. Methods* **11,** 54 (2006).

466 58. South, A. rworldmap: A new R package for mapping global data. *The R J.* **3**, 35–43 (2011)

Acknowledgement

We thank NS Jacobsen for his help with the RAM stock assessment database, CA Stock for advice on the energy fluxes, UR Sumaila for making the global fish prices available and H van Someren Gréve for figure illustrations. PDvD, ML, KHA conducted the work within the Centre for Ocean Life, a VKR center of excellence supported by the Villum Foundation. PDvD received funding from the People Programme (Marie Curie Actions) of the European Union's Seventh Framework Programme (FP7/2007-2013) under REA grant agreement no 609405 (COFUNDPostdocDTU). ML is supported by a VILLUM young investigator grant (13159). RAW acknowledges support from the Australian Research Council (Discovery project DP140101377).

Author contributions:

PDvD, ML, BRMK, KHA conceived the study. RAW contributed with fisheries landings data. PDvD performed the research with support of ML and KHA. PDvD, ML and KHA wrote the manuscript. All authors contributed to interpretation of the results and commented on the manuscript.

Author information:

The authors declare no competing financial interests. Correspondence and requests for materials should be addressed to PDvD (pdvd@aqua.dtu.dk**)**

Figure legends

Figure 1. Conceptual figure illustrating the competitive interactions between large pelagic specialists and large demersal generalists that feed on smaller pelagic and/or demersal fish and invertebrates. The smaller pelagic and demersal fish feed on zooplankton or zoobenthos. Illustration by H. van Someren Gréve.

Figure 2. Average weight fraction of large pelagic fish compared to large demersal fish in fisheries landings between 1970 and 2014. Large pelagic fish are the dominant group of fish in most tropical and subtropical areas, whereas large demersal fish are dominant in temperate regions and the exclusive group at the poles. Grey ecoregions in the map are excluded from the analysis due to limited data availability (see method section). The boxplots show the ecoregions (n=217) in bins of 5 degrees latitude, the midline of the box shows the median of the data, the limits of the box show the first and third quartile and the whiskers extend to a maximum of 1.5 times the interquartile range. The line is derived with a loess smoother.

Figure 3. Relationships between the fraction of large pelagic fishes in fisheries landings and the ratio between the fraction of net primary production (NPP) that remains in the photic zone (F_{photic}) versus the fraction that reaches the seabed (F_{seabed}) for all ecoregions with available data (n=217). Large demersal fish are dominant at approximately equal pelagic – benthic NPP ratios, while pelagic fish are dominant in areas where a high fraction of NPP remains in the photic zone (and/or where a low fraction of NPP reaches the seabed) (generalized additive model, p-value < 0.001, deviance explained = 68%). The fit is indicated by the solid line, the grey area shows the 95% confidence interval. Fish illustrations by H. van Someren Gréve.

Figure 4. Predictions of the dominance of large pelagic specialists or demersal generalists across marine ecoregions using a food-web model. **a**, Map of the predicted weight fraction large pelagic specialists compared to demersal generalists in the food-web model based on region-specific energy fluxes. **b**, Relationship between the fraction large pelagic fish in fisheries landings data and food-web model for each ecoregion ($y = 0.04 + 0.92x_1$, $r^2 = 0.58$, p-value < 0.001), coloured points correspond to ecoregions with a large difference (> 0.33) between the model predictions and the data. **c**, Map of all ecoregions with a large difference (> 0.33) between the fraction large pelagic fish in fisheries landings and the model, following (4b). Grey ecoregions are excluded from the analysis due to limited data availability. Fish illustrations by H. van Someren Gréve.

514 **Figure 1**

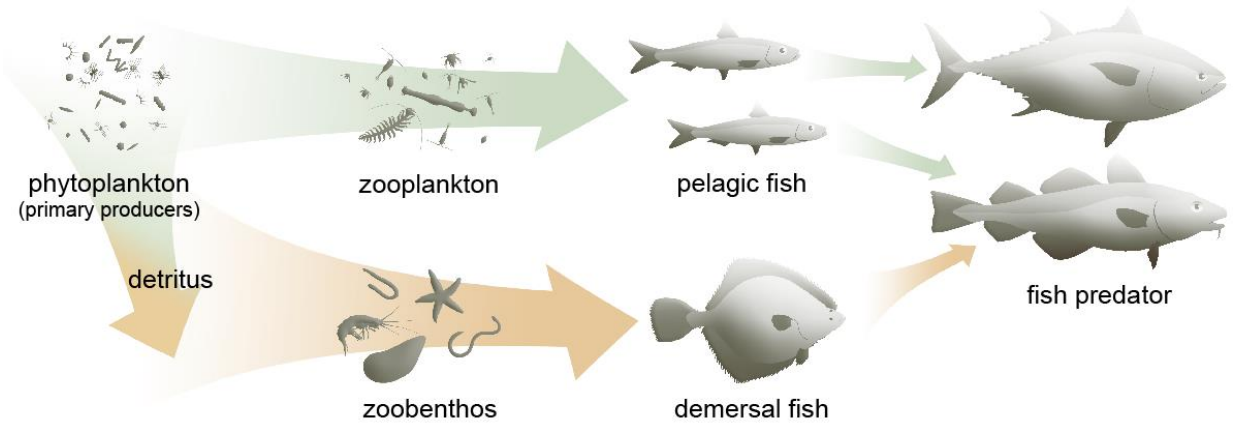

515

516

517 **Figure 2**

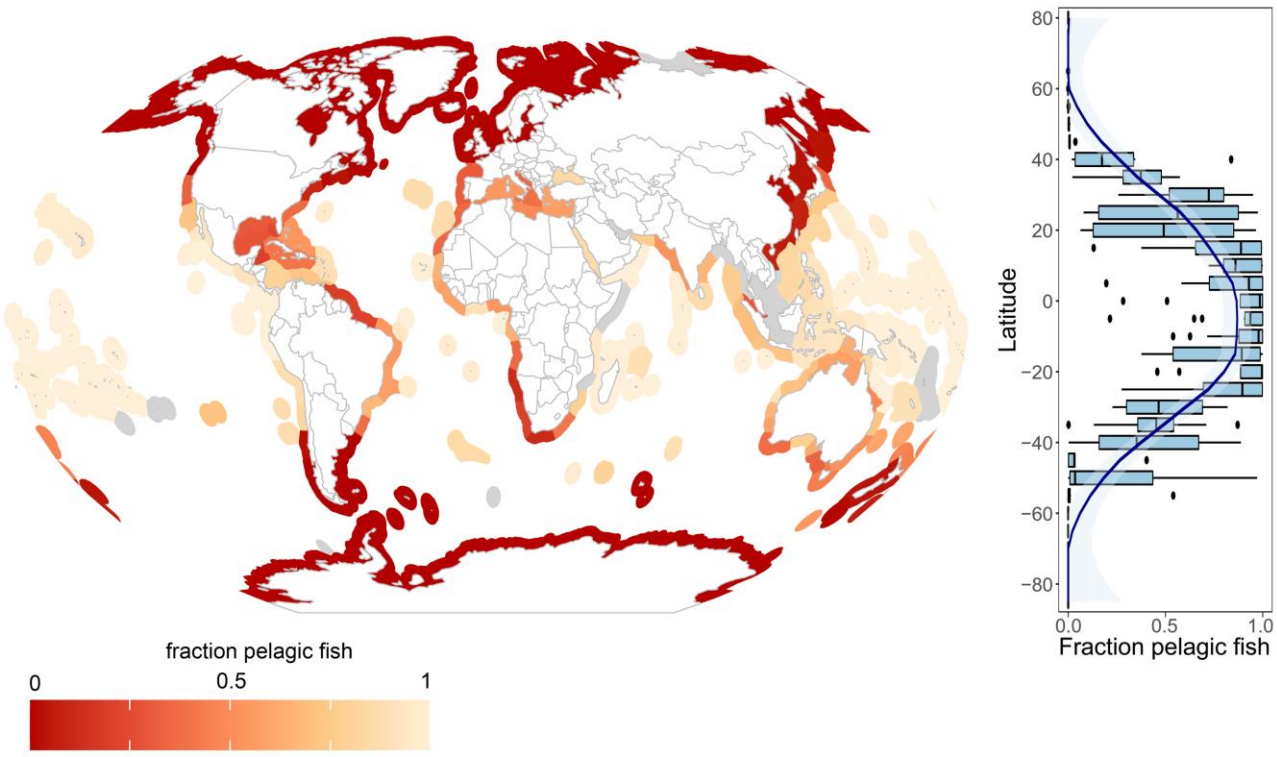

518

519

520 **Figure 3**

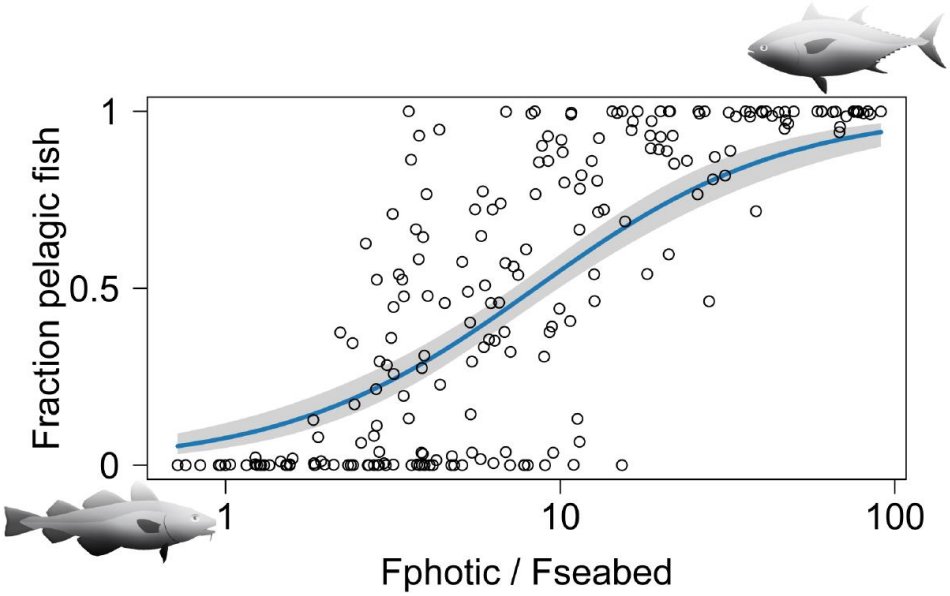

521

522

523 **Figure 4**

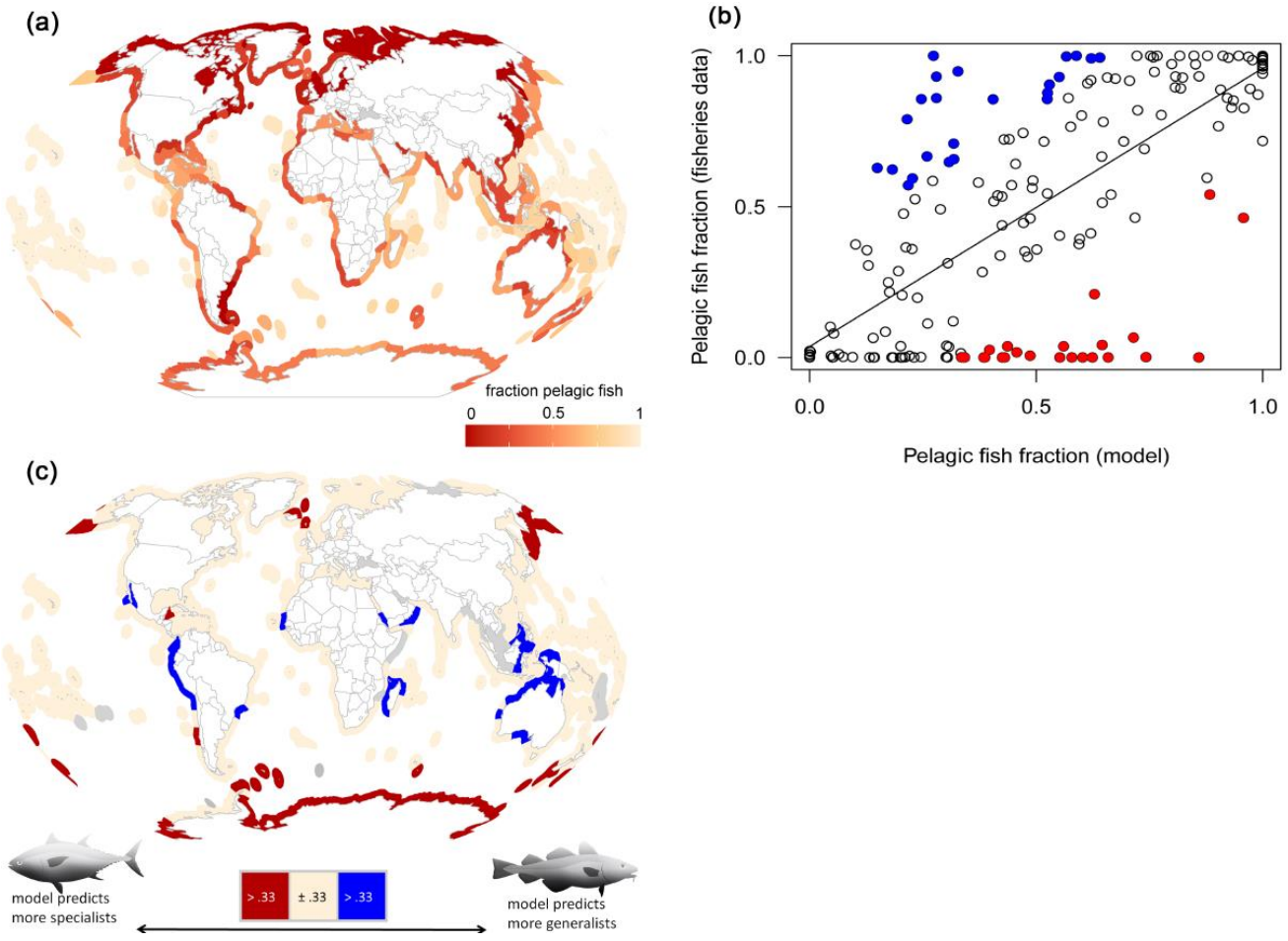

524

525